



A High Precision Study of the Coulombic Efficiency of Li-Ion Batteries

To cite this article: A. J. Smith *et al* 2010 *Electrochem. Solid-State Lett.* **13** A177

View the [article online](#) for updates and enhancements.

EXTENDED ABSTRACT DEADLINE: DECEMBER 18, 2020

 **239th ECS Meeting**
with the 18th International Meeting on Chemical Sensors (IMCS) 

May 30-June 3, 2021 **SUBMIT NOW →**



A High Precision Study of the Coulombic Efficiency of Li-Ion Batteries

A. J. Smith,^{*} J. C. Burns, and J. R. Dahn^{*,z}

Department of Physics and Atmospheric Science, Dalhousie University, Halifax, Nova Scotia B3H3J5, Canada

The capacity loss and coulombic efficiency of LiCoO₂, LiFePO₄, and LiMn₂O₄/graphite commercial Li-ion batteries have been examined using high precision coulometry. The cells were charged and discharged at different C rates and temperatures to observe trends in the aging of cells. The experiments show that time, not cycle count, is the dominant contributor to the coulombic inefficiency of Li-ion batteries cycled at low rates.

© 2010 The Electrochemical Society. [DOI: 10.1149/1.3487637] All rights reserved.

Manuscript submitted July 30, 2010; revised manuscript received August 16, 2010. Published September 13, 2010.

Li-ion batteries are used in cellular phones, laptops, camcorders, and other portable electronic devices because they have high energy density and calendar lives of at least 3–4 years, enabling them to outlive the portable electronics that they power. Industrial products such as backup power supplies, satellites, and electric vehicles require significantly longer calendar life, at least 10 years, and can operate under challenging environmental conditions. The ability of the Li-ion cells to operate under realistic conditions (i.e., long periods at elevated temperature) must be demonstrated.

Over the past 10 years, only a few published results exist that report the cell performance monitored over periods of months or years.^{1–7} The most impressive of these articles, by Broussely et al., observed the aging of cells over a period of ~4 years. They demonstrated that the capacity, power, internal pressure, and impedance of Li-ion cells are strongly dependent on calendar life.¹ By utilizing high precision coulometry, we hope to measure such effects, which would normally take years to measure, in a matter of weeks.

Here, a high precision charger (HPC)⁸ (an in-house battery cycler) was used to study the capacity retention and coulombic efficiency (CE) of common types of Li-ion cells cycled at low rates and at various elevated temperatures. The parasitic reactions that take place within Li-ion batteries consume charge at a fixed (temperature-dependent) rate at all temperatures studied, independent of the cycling rate. Consequently, cell life at elevated temperature is controlled by the time of exposure, independent of whether cells are being cycled or not.

Experimental

All cells were tested using the HPC described in Ref. 8. This device can measure the CE of cells cycled at rates lower than C/10 to a precision of ±0.02%.

Three types of commercial Li-ion cells were obtained from reputable suppliers to perform these tests. Twelve each of 18650-sized LiCoO₂/graphite cells (2400 mAh) and LiMn₂O₄/graphite (1400 mAh) cells were cycled between 3.0 and 4.2 V. Twelve 26700-sized LiFePO₄/graphite cells (2200 mAh) were cycled between 2.7 and 3.8 V. Each type of cell was cycled using applied currents of 100, 50, or 25 mA at 30.0, 40.0, 50.0, or 60.0 ± 0.1 °C. This provided a wide selection of temperatures and rates to observe trends in the behavior of the cells.

Results and Discussion

Figure 1 shows the cell potential vs capacity of the three types of commercial cells cycled with an applied current of 100 mA at 40 °C. The larger panels for each cell show the 1st, 5th, 10th, etc. cycles over the entire voltage window. The smaller insets on the left and right show the expanded views of the discharge and charge end

points, respectively, for the 2nd, 4th, 6th, 8th, and 10th cycles. The capacity axis tracks the accumulated capacity of the cells, assuming that the capacity of the cell after the very first discharge was 0.00 mAh. All end points continually move to the right as Li-ion cells are tested and this is a general feature of all cells (many are not shown in this article) we have tested at low rates.

Figure 2 shows the normalized capacities for all of the cells plotted vs cycle number. The capacity fade of all the cell chemistries increases as the temperature increases. The LiMn₂O₄ and LiFePO₄ cells cycled at lower C rates lose capacity faster than those cycled at higher C rates. The LiCoO₂ cells, however, are less affected by the cycling rate, showing a similar capacity fade vs cycle count for the different C rates at the same temperature.

The cycle life of a Li-ion cell is not infinite because small fractions of cell components are consumed by parasitic reactions during each cycle possibly creating capacity fade, electrolyte oxidation, and so on (e.g., Ref. 1). The magnitude of these parasitic reactions can be monitored by careful measurements of CE

$$CE = Q_d/Q_c = \text{charge out/charge in} \quad [1]$$

As battery manufacturers produce cells that are increasingly free of these unwanted side reactions, the CE becomes closer to unity (1.0000...) and the cells are able to cycle without loss of lithium, electrolyte decomposition, etc. In some cases, it is conceivable that anodic and cathodic side reactions are nonzero and balanced and the cell capacity would initially be stable during cycling. However, the existence of these reactions would be detected by a CE less than 1.0000 and cells would ultimately fail due to the consumption of cell components.

Figure 3 shows the CE vs cycle number for the same cells described by Fig. 2. The CE is strongly affected by temperature for all the cells, so that as the temperature increases, the CE departs more and more from unity. This is because parasitic reactions such as electrolyte oxidation and loss of Li to solid electrolyte interface growth are amplified as temperatures are elevated. Figure 3 shows that cells cycled at lower rates had CEs that are departed further from unity than cells cycled at faster rates. This is because cells cycled at lower rates have more time per cycle for parasitic reactions to occur and consume charge.

Figure 4 shows the coulombic inefficiency (1.0000 – CE) divided by the time of one charge–discharge cycle plotted vs time for the same cells described by Fig. 2 and 3. The coulombic inefficiencies per hour for cells at a given temperature are almost exactly the same at any given time, irrespective of the cycling rate, suggesting that time, not cycle count, is the dominant contributor to charge loss. This suggests that at a given temperature, parasitic reactions that cause coulombic inefficiency occur in the cells at a reaction rate that is independent of the cell cycling rate. Therefore, the amount of parasitic reactions that occur for a given cycle is simply the parasitic reaction rate multiplied by the time of one cycle. This leads to a general expression for the coulombic inefficiency of any given cycle

^{*} Electrochemical Society Student Member.

^{**} Electrochemical Society Active Member.

^z E-mail: jeff.dahn@dal.ca

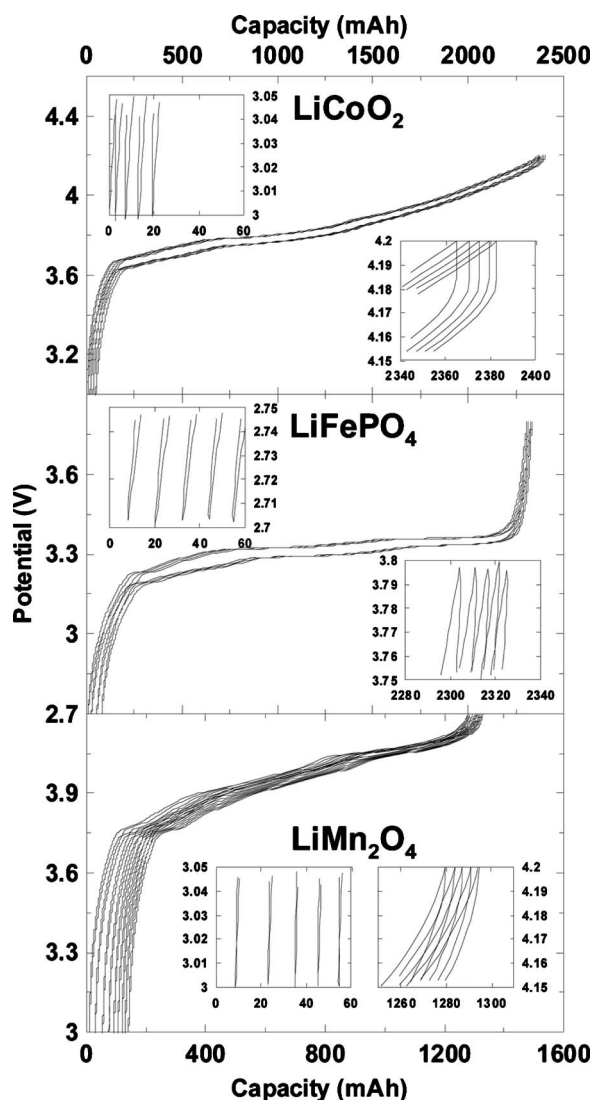


Figure 1. Voltage-capacity graphs for LiCoO₂, LiFePO₄, and LiMn₂O₄/graphite Li-ion cells charged and discharged at 100 mA at 40°C. The insets show the motion of the charge and discharge end points for every second cycle.

$$(1.0000 - \text{CE}) = k(T, t) \times (\text{time of one cycle}) \quad [2]$$

where $k(T, t)$ is the parasitic reaction rate that depends on the cell temperature (T) and calendar time (t).

Obviously, impedance growth, which can lead to capacity loss during high rate cycling, is not monitored in such low rate experiments. However, the power fade in cells tested at the same temperature for the same time (described by Fig. 2-4) is very similar because those cells each have had the same amount of parasitic loss, leading to the formation of decomposition products on electrode surfaces.

To test the model described by Eq. 2, the CE, for the same cells after ~ 600 h, is plotted vs the log of C rate in Fig. 5. As shown in Fig. 3, the CE of the cells departed more strongly from unity as the cell temperature was raised or as the cycling rates were decreased. The solid lines in Fig. 5 are curves fitted to the data using Eq. 2, where it was assumed that k is constant with time for a given temperature. These curves fit the experiments extremely well. Table I gives the values of k as a result of the curve fitting for the three cell types at the four temperatures studied. However, one cannot simply assume that increasing cycling rates indefinitely continues to im-

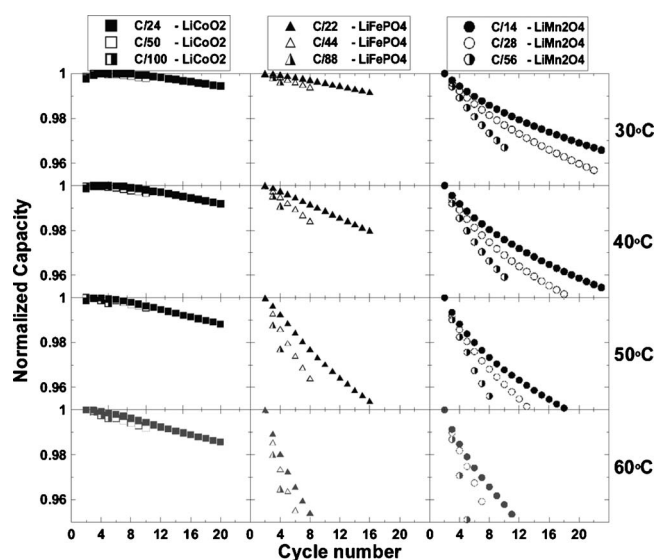


Figure 2. Normalized capacity vs cycle number of the 36 Li-ion cells charged and discharged at the C rates and temperatures indicated.

prove the CE. At a significantly high charge rate, physical phenomena like Li plating and impedance changes reduce the capacity retention and CE of the cells.

It is not the purpose of this work to compare LiCoO₂, LiFePO₄, and LiMn₂O₄ Li-ion cell technologies in terms of “better or worse” because we do not know the details of the cell assembly, electrolyte composition, etc. for the commercial cells studied here. However, clearly, the CE is controlled by cycle time at a given temperature for all three chemistries and that is the main message we want to convey.

Conclusions

The time of one cycle is the dominant contributor to the coulombic inefficiency of Li-ion batteries cycled at low rates, indicating that parasitic reactions, which consume charge, proceed independent

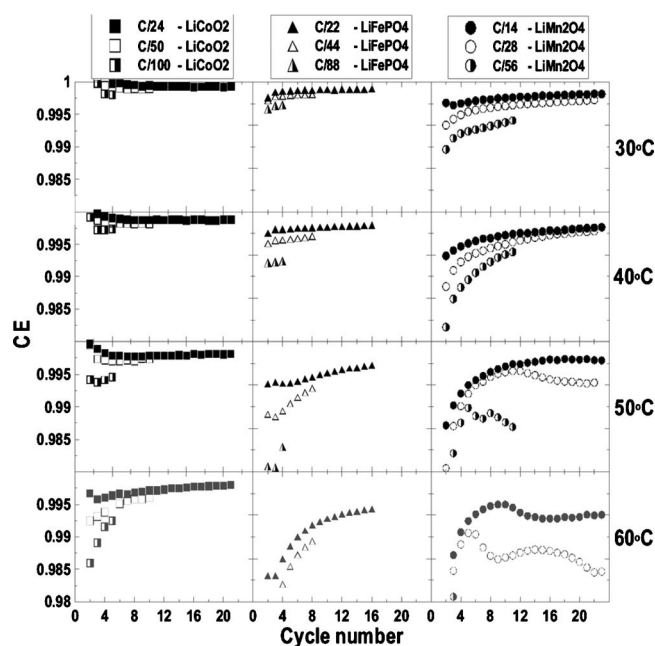


Figure 3. CE vs cycle number of the 36 Li-ion cells charged and discharged at the C rates and temperatures indicated.

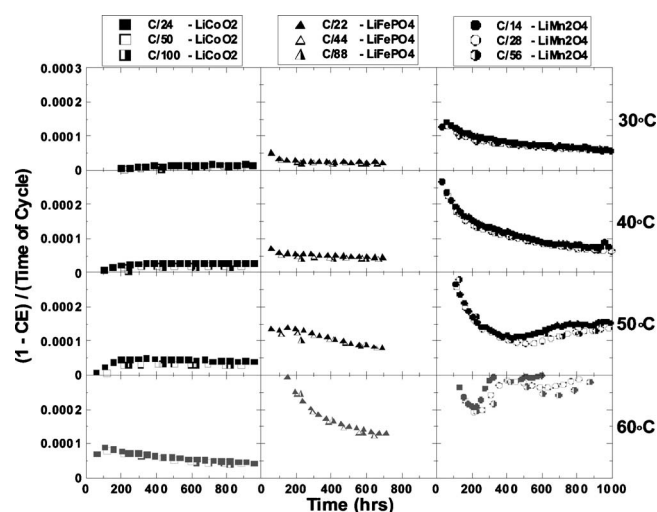


Figure 4. Coulombic inefficiency $(1.0000 - \text{CE})$ divided by time of a cycle plotted vs time for the 36 Li-ion cells charged and discharged at the C rates and temperatures indicated.

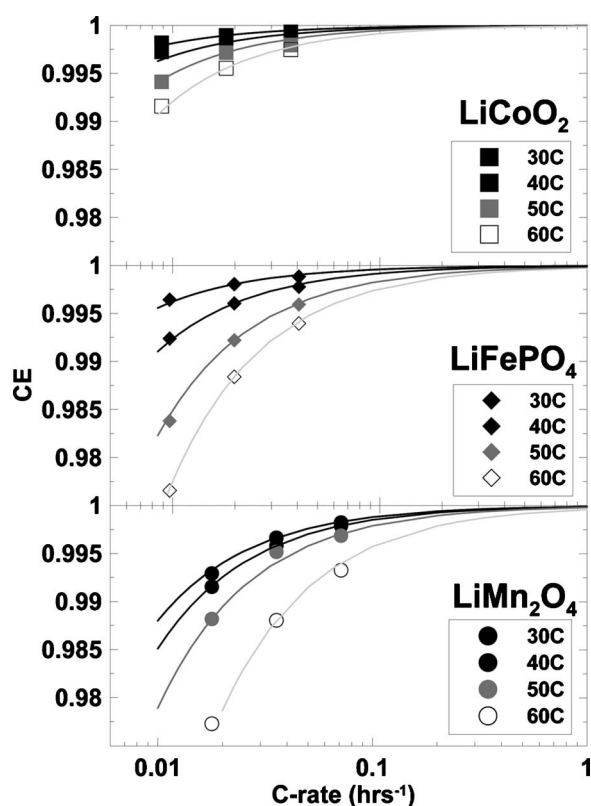


Figure 5. CE vs C rate for the 36 Li-ion cells tested at 30, 40, 50, and 60°C. The CE data were selected after 600 h of testing. The solid lines are fits of $(1.0000 - \text{CE}) = k(\text{time of one cycle})$ to the data, where k is a constant. k increases with temperature as shown in Table I.

Table I. Parasitic reaction rate (k) (h^{-1}) vs temperature for LiCoO_2 , LiFePO_4 , and LiMn_2O_4 /graphite Li-ion cells as determined from Fig. 5. The constant (k) relates the CE to the time of one cycle by $(1.0000 - \text{CE}) = k(\text{time of one cycle})$.

Temperature (°C)	Cell types		
	LiCoO_2 $k(\text{h}^{-1})$	LiFePO_4 $k(\text{h}^{-1})$	LiMn_2O_4 $k(\text{h}^{-1})$
30	0.000011	0.000022	0.000060
40	0.000019	0.000045	0.000077
50	0.000030	0.000089	0.00011
60	0.000046	0.00013	0.00021

of cycling rate at a given temperature for cells with graphite negative electrodes. These parasitic reactions slow down as cells age because the CE approaches unity, presumably due to the thickening of interface layers between the electrodes and electrolyte.

High rate cycling of Li-ion cells, as is common in accelerated testing by manufacturers, may lead to spurious conclusions about cycle life under conditions of low rate (i.e., daily) charge and discharge due to the extended time available for parasitic reactions to occur. It is believed that precision coulometry should be used more widely by Li-ion battery researchers to rapidly determine the impact of electrolyte additives, etc. on parasitic reactions in Li-ion cells.

Acknowledgments

The authors acknowledge NSERC and 3M Canada for funding this work under the auspices of the Industrial Research Chairs program. The authors thank Dr. Jamie Gardner and Dr. Bob Visser for their personal support of this project and Dr. Mark Obrovac for a critical reading of the manuscript.

Dalhousie University assisted in meeting the publication costs of this article.

References

1. M. Broussely, Ph. Biensan, F. Bonhomme, Ph. Blanchard, S. Herreyre, K. Nechev, and R. J. Staniewicz, *J. Power Sources*, **146**, 90 (2005).
2. M. Broussely, S. Herreyre, Ph. Biensan, P. Kasztajna, K. Nechev, and R. J. Staniewicz, *J. Power Sources*, **97–98**, 13 (2001).
3. K. Asakura, M. Shimomura, and T. Shodai, *J. Power Sources*, **119–121**, 902 (2003).
4. D. Aurbach, B. Markovsky, A. Rodkin, E. Levi, Y. S. Cohen, H.-J. Kim, and M. Schmidt, *Electrochim. Acta*, **47**, 4291 (2002).
5. B. Markovsky, A. Rodkin, Y. S. Cohen, O. Palchik, E. Levi, D. Aurbach, H.-J. Kim, and M. Schmidt, *J. Power Sources*, **119–121**, 504 (2003).
6. R. P. Ramasamy, R. E. White, and B. N. Popov, *J. Power Sources*, **141**, 298 (2005).
7. E. Scott, J. Brown, C. Schmidt, and W. Howard, Abstract 239, The Electrochemical Society Meeting Abstracts, Vol. 502, Los Angeles, CA, Oct 16–21, 2005.
8. A. J. Smith, J. C. Burns, S. Trussler, and J. R. Dahn, *J. Electrochem. Soc.*, **157**, A196 (2010).